Flight Testing of Laminar Flow Control in High-Speed Boundary Layers

William S. Saric & Helen L. Reed
Arizona State University
Mechanical & Aerospace Engineering Dept.
Tempe, AZ. 85287-6106 USA

saric@asu.edu ; helen.reed@asu.edu

Daniel W. Banks
NASA-Dryden Flight Research Center
Mail Stop 2288
Edwards , CA. 93524 USA

dan.banks@dfrc.nasa.gov

SUMMARY

This paper presents data from a series of laminar-flow flight tests at NASA Dryden Flight Research Center on the F-15B. It is shown that periodic discrete roughness elements near the leading can increase the laminar flow region at both supersonic and subsonic flight Mach numbers. Infra-red thermography was used to visualize laminar-turbulent transition. Although the experiment was designed for Mach 1.85, it was possible to obtain data at other Mach numbers as well. The results at Mach 1.85 and 0.911 are presented. Unfortunately, flowfield nonuniformities limited the Mach number range and the extent of observed laminar flow. The results are encouraging that periodic discrete roughness elements near the leading edge can be used as a laminar flow control technique.

1.0 INTRODUCTION

The present paper addresses laminar flow control (LFC) in swept-wing boundary layers in both high subsonic and supersonic flight. The duration of long-range supersonic flight and high-altitude UAV surveillance aircraft depends, of course, on the drag budget. Achieving laminar flow on 70 %– 80% of the wings, usually results in an overall drag reduction of 20 %– 25% and hence, extends the range or loiter time of these aircraft.

Swept-wing boundary layers are subject to crossflow instabilities that do not lend themselves easily to prediction and control [1,2]. Delaying the pressure minimum and accelerating the boundary layer stabilizes streamwise instabilities (T-S waves) but destabilizes crossflow waves. In low-disturbance environments, one can expect that stationary crossflow waves will dominate. In this case, an innovative technique using periodic discrete roughness elements (DRE) has been shown to stabilize stationary crossflow waves [3, 4, 5] in lowspeed flows.

The basic idea is as follows. The crossflow instability has a frequency response that includes both traveling and stationary waves. In low-turbulence environments, the dominant mode appears as stationary waves that are excited by micron-sized surface roughness [2]. These stationary waves are in the form of streamwise-

Paper presented at the RTO AVT Specialists' Meeting on "Enhancement of NATO Military Flight Vehicle Performance by Management of Interacting Boundary Layer Transition and Separation", held in Prague, Czech Republic, 4-7 October 2004, and published in RTO-MP-AVT-111.

oriented, co-rotating vortices. Given a random roughness distribution of a normal surface, one observes stationary waves at a wavelength predicted by linear theory to be the most unstable wavelength. This *critical* wavelength, λ_{crit}, will grow and also generate harmonics in wavenumber space ($\lambda_{crit}/2, \lambda_{crit}/3, \text{etc}$) but not subharmonics ($2\lambda crit, 3\lambda crit, etc.$). Since these are stationary streamwise vortices, the weak rotational components convect streamwise momentum and modify the mean flow in a nonlinear sense. This modified mean flow has different stability characteristics than the unmodified flow. If one introduces a subcritical *control* wavelength, λ_{cntrl}, where the control wavelength is about 50% - 60% of λ_{crit}, stationary waves will grow at this wavelength and inhibit the growth of the most unstable stationary disturbance. Since the mean flow is now spanwise periodic at this wavelength, traveling disturbances are also restricted to less unstable modes. The comparisons between experiment [3], nonlinear parabolized stability equations (NPSE) [4], and direct numerical simulation (DNS) [5] show outstanding agreement. The airfoil design process using distributed roughness is given by Saric & Reed [6]. Since the basic background material on crossflow-induced transition is in references [1, 2], the details of the laminarization technique are in references [3, 4, 5], and the implementation and airfoil design process is given in [6, 7], there is no need to repeat the standard references.

2.0 DESCRIPTION OF THE FLIGHT EXPERIMENT

The flight experiment utilizes a wing model mounted underneath the F-15B aircraft at NASA Dryden Flight Research Center (DFRC). The model, shown in Figure 1, is a trapezoid with a 30º leading edge sweep and a -15º trailing edge sweep. The profile is a modified bi-convex with a mid-span chord of 0.762 m (2.5 ft). Before modification, this model was first tested by Richard Tracy and his colleagues at Reno Air to achieve laminar flow with the 15º leading edge sweep.

Figure 1: 30º leading-edge-sweep model under the F-15

The flight objective is to achieve Mach 1.85 and a unit Reynolds number of 13.1×10^6/m (4×10^6/ft) for a nominal chord Reynolds number of 10×10^6. The aircraft was limited to a maximum dynamic pressure ($\bar{q}_{max}$) of 1200 psf. The designed flight trajectory is shown in Figure 2. Some modifications were incorporated as temperature conditions changed throughout the year and occasionally we were unable to achieve $\bar{q}_{max}$.

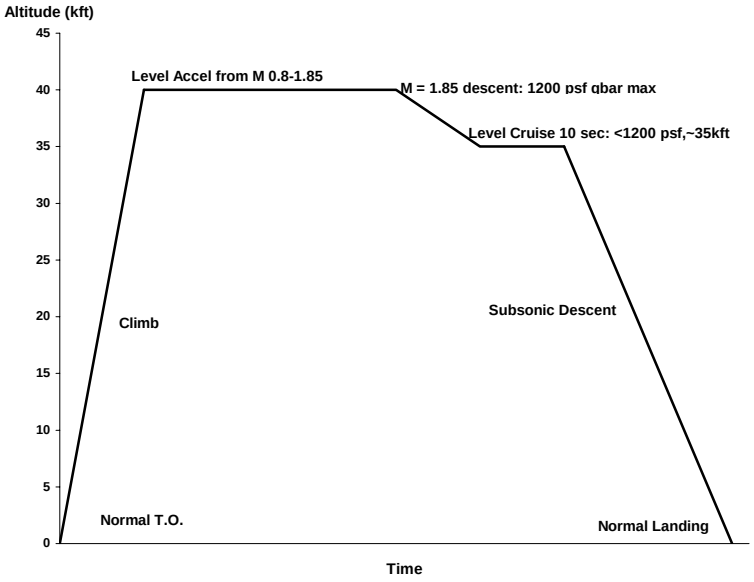

Figure 2: Flight trajectory

Complete Euler calculations were done on the aircraft/model at flight Mach numbers. The pressure contours are shown in Figure 3. There is some spanwise nonuniformity but the model seems to be shock free at this Mach number.

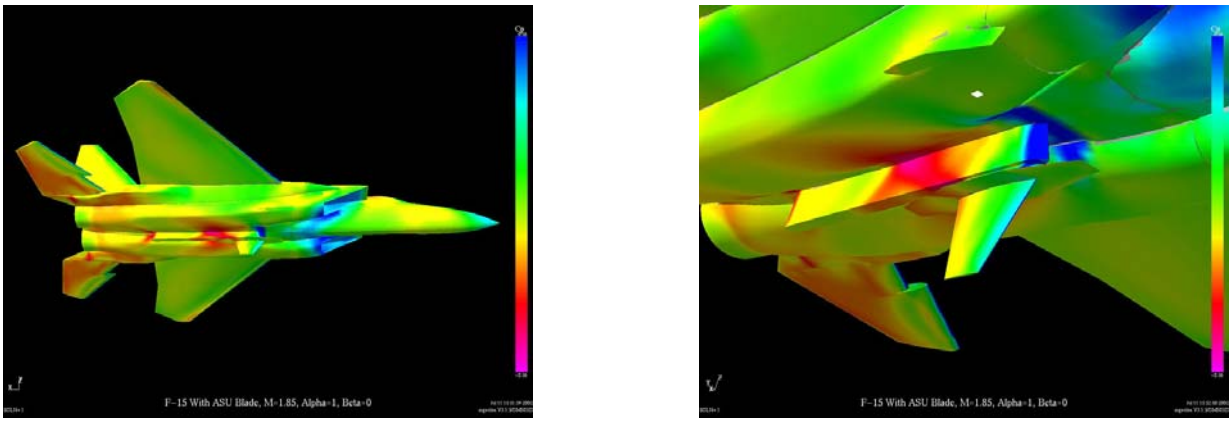

Figure 3: Pressure contours from Euler calculations of F-15B at Mach 1.85

The most revealing result from these calculations is the visualization of a bleed-over shock from the pylon that intersects the model when the Mach number is less than 1.8. This shock trips the boundary layer making LFC ineffective. All of the supersonic measurements had to be conducted at Mach numbers greater than 1.8. The calculations further show that there is some aircraft induced downwash that changes the effective sweep angle across the span of the model. Thus the local flow sweep angle varied from approximately 35 degrees at the root to 30 degrees at the tip.

The model chord varies from 1.2 m (47.36 in) at the root to 0.55 m (21.79 in) at the tip. The nominal chord is 0.9 m (35.58 in), the span is 0.78 m (30.75 in), the thickness is 3.4%, and the nose radius is 5 mm (0.2 in). The attachment line Re_θ is always less than 70. The pressure distributions from the Euler calculations are shown in Figure 4.

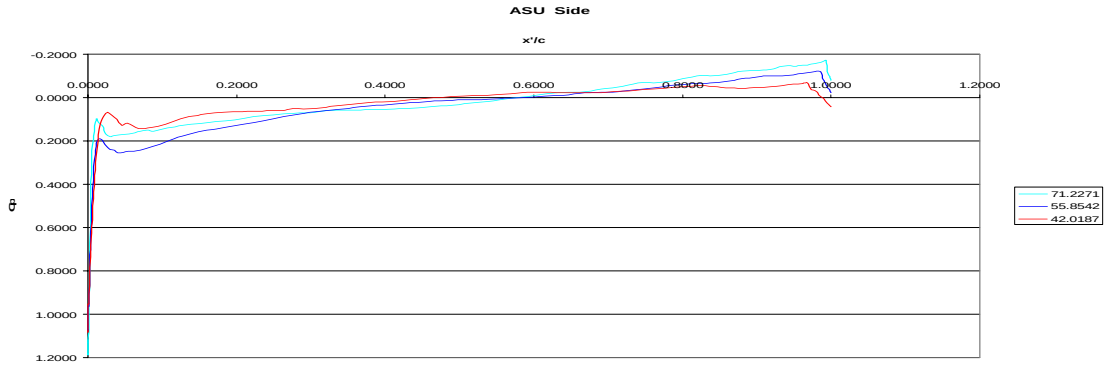

Figure 4: $-C_P$ distribution at three span locations

Note the suction peak near the leading edge that seems to be larger inboard. This in fact destabilizes the boundary layer in a manner that was not accounted for in the design using FLO-87. The stability calculations (Figures 5 and 6) were actually done using the pressures calculated in Figure 4.

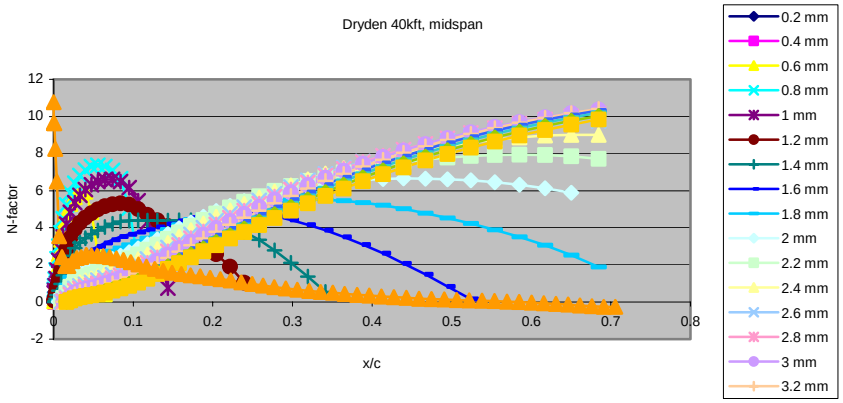

Figure 5: N-factor calculations at mid-span, 40 kft, and, M = 1.85

The N-factor calculations of Figure 5 are for stationary crossflow vortices at the wavelengths indicated in the right-hand column. It shows large early growth of the 0.8 and 1.0 mm waves. This is unexpected from the earlier design points because the aircraft interference was not taken into account. It does appear that the 4 mm wave is the most unstable and one that would lead to transition.

Figure 6 shows the N-factors calculations in the outboard region. Here the initial growth of the short waves, 0.6 mm to 1.0 mm, is reasonable and more like the design case. We still have the 4 mm wave as the most unstable (not shown in Figure 6) and the 2 mm wave for control. The N-factors of Figure 6 increase as $\overline{q}_{max}$ is reached at 35 kft.

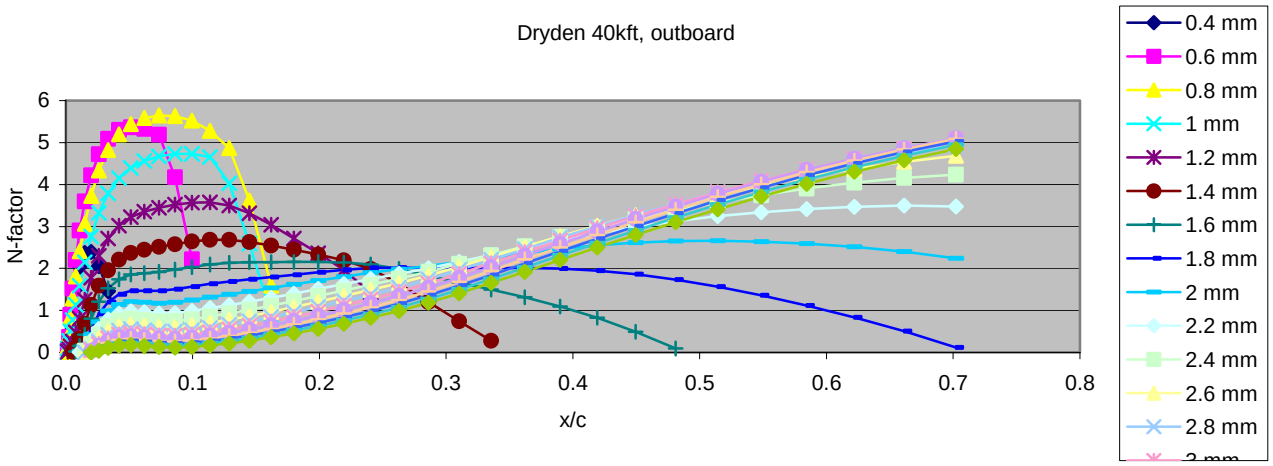

Figure 6: Outboard N-factor calculations at 40 kft, and, *M* = 1.85

3.0 RESULTS

Infra-Red Thermography (IRT) is used as the primary instrumentation for detecting transition location. A limited number of surface pressure and temperature measurements are also recorded. The measured and calculated pressures agreed but there were not enough pressure ports to resolve the early suction peak. Unfortunately, we were unable to implement the ASU-designed freestream fluctuating pressure measurement.

3.1 Subsonic Results

The IR camera was operative throughout the flight trajectory so that selected subsonic points could also be used for data. As mentioned earlier, no supersonic results were valid for mach numbers less than 1.8. The criteria used for choosing subsonic data was that the model was not thermally saturated and conditions were held for at least two seconds. The principal test conditions were:

Mach = 0.911; Altitude = 9245 m (30,417 feet); Temperature = 235 K (-36 F)

unit Reynolds number = 8.1×10^6/m (2.46×10^6/ft); mid-span chord Reynolds number = 6.15×10^6

The periodic discrete roughness elements (DRE) had the following characteristics: diameter = 1 mm; height = 6 μm (0.00024 inch); spacing = 4 mm. Figure 7 is a IRT image showing full-chord laminar flow under the stated conditions. In Figure 7, the light area is laminar, the dark area is turbulent. The two turbulent wedges at 1/3 and 2/3 span are due to out-gassing pressure ports. *The boundary layer is otherwise laminar.* In the case *without* the DRE, transition was observed (and also predicted) to be caused by T-S waves at 70% chord because of the very sharp pressure recovery. The DRE spacing was the critical spacing for Mach = 1.85 but at the stated conditions, this crossflow wavelength grew only modestly. The growth of the stationary crossflow wave did however modify the meanflow thereby restricting the growth of the T-S wave. Thus, the boundary layer remained laminar through the pressure minimum. It appears therefore that the distributed roughness can also favorably influence traveling T-S waves as well by making the basic state spanwise periodic. This offers an unexpected benefit of using DRE.

Figure 7: R Image of model at M = 0.911 Conditions stated in text.

3.2 Supersonic Results

A total of 11 flights were scheduled from spring 2002 through the summer of 2003. Of these, 6 were aborted for various technical reasons. The data presented here are from the summer of 2003. Additional tests were planned but funding issues terminated the program. Figure 8 contains a composite of the IRT results from a typical supersonic flight. In this case, laminar flow is dark and turbulent flow is light. The principal test conditions are: Mach = 1.85; Altitude = 12 km (40 kft); unit Re = 11.8 x 10^6/m (3.6 x 10^6/ft); mid-span chord Rec =9 x 10^6

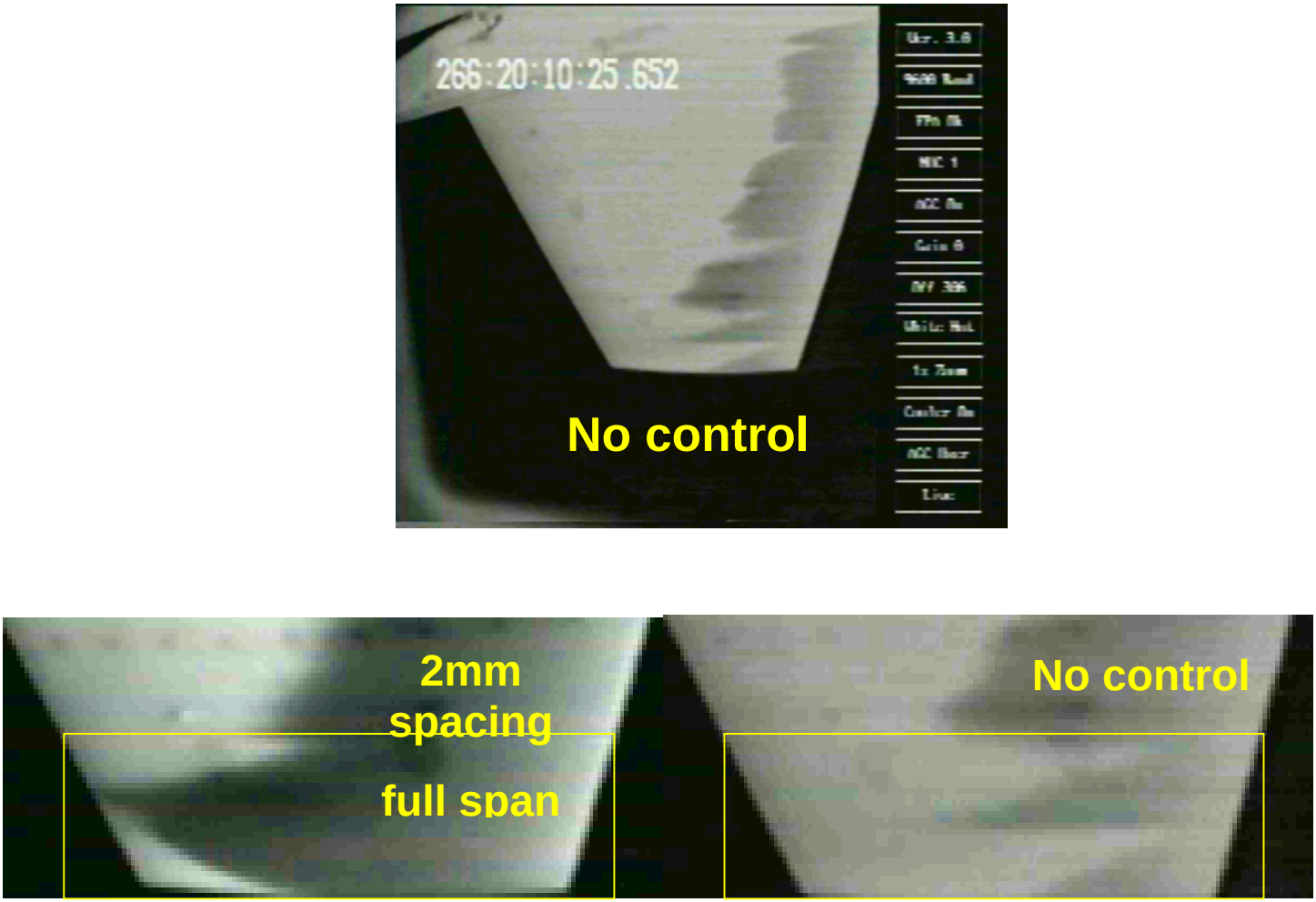

Figure 8: Supersonic IRT Results. Upper figure is entire model with no control roughness. The lower two figures are enlargements of the outboard region.

Close examination of the outboard region showed an increase in laminar flow when 0.75 mm diameter DRE were placed on 2 mm centers. The most unstable wave was at 4 mm. The DRE height was 6 microns. However, control was observed only in the outboard region. The higher than anticipated inboard suction peak and sweep angle obviated the control inboard. The suction peak also caused an increased sensitivity to roughness nonuniformities. Because of the unusually high temperatures during the summer of 2003, it was not

possible to achieve the design chord Reynolds number. Typically, Mach 1.85 was achieved at 40 kft only at the end of the supersonic corridor and the downhill portion of the trajectory to 35 kft could not be obtained.

4.0 SUMMARY

The chord Reynolds numbers for the supersonic case are lower than most supersonic applications, but demonstrate the possibility of the DRE laminarization concept in supersonic flow (higher-Reynolds-number, wind-tunnel results are given in [6]). The difficulties with this experiment demonstrate the need to always do a full computation of the flowfield. The underside of the F-15B did not have the anticipated uniform flowfield. Had this been known early enough, the model would have had a much different design.

The chord Reynolds numbers in the high subsonic case is representative of high-altitude UAV surveillance aircraft and thus, these data have a direct application. These results encourage additional flight-test work with DRE in both T-S and crossflow dominated regimes. Additional wind-tunnel experiments in the case of crossflow must be limited to facilities with extremely low turbulence levels.

ACKNOWLEDGEMENTS

The work was supported by the DARPA QSP program under Grant MDA972-01-2-0001 and by NASA-DFRC. The authors gratefully acknowledge the use of FLO-87 from Drs. Anthony Jameson and Juan Alonso of Stanford University and the F-15 Euler calculations by Richard Tracy and Jason Matisheck of Reno Air. Andrew Carpenter of ASU assisted in the latter part of the program. Thanks go to David Richwine and the staff of DFRC for all of the conscientious work needed to make this happen.

REFERENCES

[1] Reed HL, Saric WS, Arnal D. 1996. Linear stability theory applied to boundary layers. *Ann. Rev. Fluid Mech.* 28:389-428

[2] Saric, WS, Reed, HL, White, EB. 2003. Stability and Transition of Three-Dimensional Boundary Layers. *Ann. Rev. Fluid Mech.* 35:413-28

[3] Saric WS, Carrillo RB Jr, Reibert MS. 1998. Nonlinear stability and transition in 3-D boundary layers. *Meccanica* 33:469-87

[4] Haynes TS, Reed HL. 2000. Simulation of swept-wing vortices using nonlinear parabolized stability equations. *J. Fluid Mech.* 405:325-49

[5] Wassermann P, Kloker M. 2002. Mechanisms and control of crossflow-vortex induced transition in a three-dimensional boundary layer. *J. Fluid Mech.* 456:49-84

[6] Saric WS, Reed HL. 2002. Supersonic laminar flow control on swept wings using distributed roughness. *AIAA Paper No. 2002-0147*

[7] Saric WS, Reed HL. 2003. Crossflow instabilities: Theory and Technology. *AIAA Paper No. 2003-0771*